IEEE Access
Multidisciplinary | Rapid Review | Open Access Journal

Received June 30, 2019, accepted July 16, 2019, date of publication July 26, 2019, date of current version August 14, 2019.

Digital Object Identifier 10.1109/ACCESS.2019.2931454

Range-Restricted Surface Interpolation Using Rational Bi-Cubic Spline Functions With 12 Parameters

SAMSUL ARIFFIN ABDUL KARIM[1,2], AZIZAN SAABAN[3], AND VACLAV SKALA[4]
[1]Fundamental and Applied Sciences Department, Universiti Teknologi PETRONAS (UTP), Seri Iskandar 32610, Malaysia
[2]Centre for Smart Grid Energy Research (CSMER), Institute of Autonomous System, Universiti Teknologi PETRONAS, Bandar Seri Iskandar, Seri Iskandar 32610, Malaysia
[3]College of Arts and Sciences, Universiti Utara Malaysia, UUM Sintok 06010, Malaysia
[4]Department of Computer Science and Engineering, Faculty of Applied Sciences, University of West Bohemia, CZ 306 14 Pilsen, Czech Republic

Corresponding author: Samsul Ariffin Abdul Karim (samsul_ariffin@utp.edu.my)

This work was supported by Universiti Teknologi PETRONAS (UTP) through Spline Triangulation for Spatial Interpolation of Geophysical Data under Grant YUTP: 0153AA-H24.

ABSTRACT This paper discusses the constraint data interpolation or range restricted interpolation for surface data arranges on rectangular meshes that lie above or below an arbitrary plane and between two arbitrary planes by using partially blended rational bi-cubic spline function with 12 parameters. Common research in range restricted surface interpolation is to construct the constrained surface lie above linear plane. However, in this paper, we consider the constraint surfaces up to degree three (cubic). To construct the constrained surface with shape preserving properties, i.e., the resulting surface will lie below or above single planes or between two respective planes, the data dependent sufficient conditions are derived on four parameters; meanwhile, the remaining eight parameters are free parameters to change the shape of the interpolating surface locally. The proposed scheme is tested with various types of data test, including some well-known functions. From the numerical results, we found that the proposed scheme is easy to use, locally control via free parameters, and require less computation compared with some existing schemes as well as visually pleasant for visualization. Furthermore, based on root mean square error (RMSE) and coefficient of determination (R^2), the proposed scheme is better than existing scheme with the value of R^2 achieved is in between 0.9701 (97.01%) and 0.9954 (99.54%). This is quite good for range restricted surface data interpolation since we can explain at least 97.01% of the variance in the interpolation by using the proposed scheme. Furthermore, the proposed scheme requires less CPU time (in seconds) compared with the existing scheme.

INDEX TERMS Constrained surface, shape preserving, interpolation, rational bi-cubic spline, local control, constraint planes.

I. INTRODUCTION

Data constrained interpolation or range restricted interpolation is an important task in the field of scientific visualization and computer graphics. Generally speaking, it is a generalization of the positivity preserving interpolation. The interpolating curves may lie between two straight lines and above or below arbitrary straight line or quadratic curves. Meanwhile in the constrained surface interpolation, researcher have considered the surface that lie above or below space plane. In order to obtain the constrained curve and surface, the sufficient condition is derived on the parameters that appeared in the description of the rational interpolant. The interpolant can be either non-rational or rational i.e. for non-parametric interpolation. There are many applications for data constrained modeling. For instance, robotic movements, medical imaging, surfaces with branches are examples of range restricted problems (Goodman *et al.* [15]). Medical imaging also involving some range restricted interpolation problems especially in image zooming and refining of body parts etc. ([25]).

In literature there are many authors that have discussed the constrained data interpolation. For instance, Abbas *et al.* [1] studies the constrained curve and surface interpolation by

The associate editor coordinating the review of this manuscript and approving it for publication was Ming Luo.

 This work is licensed under a Creative Commons Attribution 4.0 License. For more information, see http://creativecommons.org/licenses/by/4.0/

using rational cubic spline (cubic/cubic) with three parameters. Asim and Brodlie [2] discussed the positivity preserving of cubic Hermite spline by inserting one or two extra knots on each sub-interval where the negativity is found. Asim *et al.* [3] studied the use of Shepard method for constrained curve interpolation. Meanwhile Brodlie *et al.* [5], [6] have discussed the positivity and constrained data visualization by using bi-cubic spline defined function over a rectangular mesh and Shepard interpolation family for scattered data for any dimensionality. Surface interpolation also has been considered in Constantini and Fontanella [10] and Hussain and Sarfraz [16]. Chan and Ong [9] used cubic Bezier triangular interpolant to interpolate range restricted scattered data. The interpolating surface is constructed by using convex combination from three local schemes comprising cubic Bezier triangular patches. Duan *et al.* [12] and Duan *et al.* [11] discussed the constrained interpolation (including convexity preserving) by using rational cubic spline (cubic/linear) with two parameters. Zhang *et al.* [26] has constructed the region constraint interpolating surfaces either lie below or above plane. Their bivariate spline is based on the true value of the function and its partial derivatives. The main weakness is that their scheme is global and does not allow the local shape manipulation as well as no flexibility for geometric visualization, since there are no free parameters.

Hussain and Hussain [17] discussed the positivity and data constrained interpolation by using rational cubic spline (cubic/quadratic) with two parameters. They claim their scheme produce the surface with C^1 continuity but without any free parameters. Hussain *et al.* [18] has studied the visualization of constrained data by using rational cubic spline (cubic/cubic). The resulting interpolating surfaces lying above space plane and their schemes have four free parameters. One of the weakness of Hussain *et al.* [18] scheme is that the first partial derivatives cannot be zero otherwise the scheme cannot be applied to construct the positive surfaces as well as the constrained surfaces above linear plane. Hussain *et al.* [19] scheme is not C^1 continuity. Shaikh *et al.* [23] studied the constrained surface construction by using rational cubic spline (cubic/quadratic) with eight parameters without any free parameters.

Walther and Schmidt [24] has studied the range restricted surface interpolation by Gregory's rational cubic spline. In their study, they give a larger condition for positivity preserving. Based on the literature review, in this study, we will have discussed the range restricted data interpolation by extending the work of Karim and Kong [21] and Karim *et al.* [22]. The proposed scheme does not involve any trigonometric function as appear in the work of Ibraheem *et al.* [20]. Furthermore, in this study, we discuss the range restricted data interpolation for surface data that lie below or above any planes up to degree three; not just above linear plane as discussed in Abbas *et al.* [1], Hussain and Hussain [17] and Shaikh *et al.* [23]. We also consider the problem when the surface lies between two arbitrary planes. These types of problems have been not discussed in early studied in the literature. Therefore, the present study has the objective to fill the gaps from existing schemes to produce constrained surface below arbitrary plane as well as between two planes.

The main outcome of the present study is listed as follows:

(a) The proposed scheme is tested for constraint surface up to degree three (linear, quadratic and cubic planes). Meanwhile in Abbas *et al.* [1], Hussain and Hussain [17] and Shaikh *et al.* [23], they only consider the constrained surface above linear plane.
(b) The proposed scheme can be used whether the first partial derivatives are given or not. Meanwhile Zhang *et al.* [25], [26] scheme only work if the first partial derivative is given at the respective knots.
(c) In line with the works of Hussain and Hussain [17], Abbas *et al.* [1] and Shaikh *et al.* [23], the proposed scheme also work both for equally and unequally spaced data set but Zhang *et al.* [25], [26] and Duan *et al.* [11]–[13] only work for equally spaced data sets.
(d) The proposed scheme in this study has the form of cubic/quadratic while Abbas *et al.* [1] has the form of cubic/cubic. Furthermore, the proposed scheme has eight free parameters for shape modification meanwhile there are no free parameters in the works of Shaikh *et al.* [23] and Hussain and Hussain [17].
(e) Knots insertions are not required as happened in Butt and Brodlie [7] and optimization based problem also is avoided. Meanwhile, Brodlie *et al.* [6] scheme requires optimization method in order to produce the constrained surface interpolation.

LIST OF ABBREVIATION

3D	*Three Dimensional*
AMM	*Arithmetic Mean Method*
CPU	*Central Processing Unit*
R^2	*Coefficient of Determination*
RMSE	*Root Mean Square Error*

LIST OF SYMBOLS

$s_i^{(1)}(x_i)$	*First derivative with respect to x at* $x = x_i$
$F_{i,j}^x$	*Partial derivative with respect to x at* (x_i, y_j)
$F_{i,j}^x$	*Partial derivative with respect to y at* (x_i, y_j)
$F_{i,j}^{xy}$	*Mixed Partial derivative at* (x_i, y_j)
$S(x, y)$	*Bi-cubic partially blended rational function over rectangular meshes*
$\alpha_{i,j}$, $\beta_{i,j}$, $\alpha_{i,j+1}$, $\beta_{i,j+1}$, $\hat{\alpha}_{i,j}$, $\hat{\alpha}_{i+1,j}$, $\hat{\beta}_{i,j}$, $\hat{\beta}_{i+1,j}$ and $\eta_{i,j}$, $\varepsilon_{i,j}$, $\delta_{i,j}$, $\chi_{i,j}$	*Free parameters*

$h_i = x_{i+1} - x_i$,
$\hat{h}_j = y_{j+1} - y_j$, Step size in x/y directions.
$\Delta_{i,j} = \frac{f_{i+1}-f_i}{h_i}$,
$\hat{\Delta}_{i,j} = \frac{f_{i,j+1}-f_{i,j}}{\hat{h}_j}$ Gradients

The remainder of the paper is organized as follows. Section 2 is devoted for Derivative Estimation. The bivariate rational bi-cubic spline is reviewed in Section 3. Meanwhile, Section 4 discuss the data constrained by using bivariate rational bi-cubic spline. Numerical results will be presented in Section 5 including the comparison with existing schemes in terms of RMSE, R^2, CPU times (s) as well as graphically. Finally, a summary and conclusions are given in Section 6.

II. DERIVATIVE ESTIMATION

The partial derivatives $F^x_{i,j}$, $F^y_{i,j}$ and $F^{xy}_{i,j}$, $i = 01, \ldots, n$ and $j = 0, 1, \ldots, m$ for 3D data can be calculated by using Arithmetic Mean Method (AMM). The details are given as follows (Hussain *et al.* [18]):

$$F^x_{0,j} = \Delta_{0,j} + \left(\Delta_{0,j} - \Delta_{1,j}\right)\frac{h_0}{(h_0+h_1)},$$
$$F^x_{n,j} = \Delta_{n-1,j} + \left(\Delta_{n-1,j} - \Delta_{n-2,j}\right)\frac{h_{n-1}}{(h_{n-1}+h_{n-2})},$$
$$F^x_{i,j} = \frac{\Delta_{i,j}+\Delta_{i-1,j}}{2}, \quad i = 1, 2, \ldots, n-1, \quad j = 0, 1, \ldots, m$$
$$F^y_{i,0} = \hat{\Delta}_{i,0} + \left(\hat{\Delta}_{i,0} - \hat{\Delta}_{i,1}\right)\frac{\hat{h}_0}{\left(\hat{h}_0+\hat{h}_1\right)}$$
$$F^y_{i,m} = \hat{\Delta}_{i,m-1} + \left(\hat{\Delta}_{i,m-1} - \hat{\Delta}_{i,m-2}\right)\frac{\hat{h}_{m-1}}{\left(\hat{h}_{m-1}+\hat{h}_{m-2}\right)},$$
$$F^y_{i,j} = \frac{\hat{\Delta}_{i,j}+\hat{\Delta}_{i,j-1}}{2}, \quad i = 0, 1, 2, \ldots, n, \quad j = 1, 2, \ldots, m-1$$

and

$$F^{xy}_{i,j} = \frac{F^y_{i+1,j} - F^y_{i-1,j}}{h_{i-1}+h_i} + \frac{F^x_{i,j+1} - F^x_{i,j-1}}{\hat{h}_{j-1}+\hat{h}_j},$$

for $i = 1, 2, \ldots, n-1, j = 1, 2, \ldots, m-1$.
where

$$h_i = x_{i+1} - x_i, \quad \hat{h}_j = y_{j+1} - y_j,$$

and

$$\Delta_{i,j} = \frac{f_{i+1}-f_i}{h_i}, \quad \hat{\Delta}_{i,j} = \frac{f_{i,j+1}-f_{i,j}}{\hat{h}_j}.$$

III. REVIEW OF RATIONAL CUBIC AND BI-CUBIC SPLINE INTERPOLANT

This section give the brief review of rational cubic spline (cubic/quadratic) with three parameters initially proposed by Karim and Kong [21]. The rational cubic spline is defined as follows:

Given functional data $\{(x_i, f_i), i = 0, 1, \ldots, n\}$ and first derivatives $d_i, i = 0, 1, \ldots, n$ such that $x_0 < x_1 < \ldots < x_n$. Let $h_i = x_{i+1} - x_i$, $\Delta_i = (f_{i+1} - f_i)/h_i$ and$\theta = (x - x_i)/h_i$ where $0 \leq \theta \leq 1$.

For $x \in [x_i, x_{i+1}], i = 0, 1, 2, \ldots, n-1$

$$s(x) \equiv s_i(x) = \frac{P_i(\theta)}{Q_i(\theta)}, \tag{1}$$

where

$$P_i(\theta) = A_0(1-\theta)^3 + A_1\theta(1-\theta)^2 + A_2\theta^2(1-\theta) + A_3\theta^3,$$
$$Q_i(\theta) = (1-\theta)^2\alpha_i + \theta(1-\theta)(2\alpha_i\beta_i+\gamma_i) + \theta^2\beta_i.$$

The rational function in (1) satisfy C^1 continuity:

$$s(x_i) = f_i, \quad s(x_{i+1}) = f_{i+1},$$
$$s^{(1)}_i(x_i) = d_i, \quad s^{(1)}_i(x_{i+1}) = d_{i+1}, \tag{2}$$

It can be shown that, the unknowns $A_i, i = 0, 1, 2, 3$ are given as follows:

$$A_0 = \alpha_i f_i,$$
$$A_1 = (2\alpha_i\beta_i + \alpha_i + \gamma_i)f_i + \alpha_i h_i d_i,$$
$$A_2 = (2\alpha_i\beta_i + \beta_i + \gamma_i)f_{i+1} - \beta_i h_i d_{i+1}.$$
$$A_3 = \beta_i f_{i+1}.$$

where $s^{(1)}_i(x)$ denotes the first derivative of $s(x)$ with respect to x and d_i denotes the derivative value which is given at the knot $x_i, i = 0, 1, 2, \ldots, n$. The parameters are chosen such that $\alpha_i > 0$, $\beta_i > 0$ and $\gamma_i \geq 0$. When $\alpha_i = \beta_i = 1$ and $\gamma_i = 0$, the rational cubic interpolant in (1) is reduced to cubic Hermite spline (Karim and Kong [21]).

A. CONSTRAINED DATA MODELING

Given the data sets(x_i, f_i), $i = 0, 1, \ldots, n$ that lying above the straight line $y = mx + c$, such that

$$f_i > mx_i + c, \quad i = 0, 1, \ldots, n. \tag{3}$$

Karim and Kong [21] have developed the following results for data lying above arbitrary straight line sets given in (3):

Theorem 1 [21]: The piecewise C^1 rational cubic spline interpolant $s(x)$ defined by (1) preserves the shape of the data that lies above the straight line $y = mx + c$, if in each subinterval $[x_i, x_{i+1}]$, $i = 0, 1, \ldots, n-1$, the parameters α_i, β_i and γ_i satisfy the following sufficient condition:

$$\alpha_i, \beta_i > 0,$$
$$\gamma_i = \upsilon_i + \text{Max}\left\{0, \frac{\alpha_i(-h_i d_i + b_i - f_i)}{f_i - a_i}, \frac{\beta_i(h_i d_{i+1} + a_i - f_{i+1})}{f_{i+1} - b_i}\right\} \tag{4}$$

where $\upsilon_i > 0$, $a = mx_i + c$, $i = 0, 1, \ldots, n-1$ and $b = mx_{i+1} + c$, $i = 0, 1, \ldots, n-1$.

TABLE 1. Data from [4].

i	0	1	2	3	4	5	6
x_i	1	1.25	2.8	3	3.2	4.2	4.5
f_i	2.5	1.5	2	2.5	3.5	4.5	5.5

TABLE 2. Numerical results.

i	0	1	2	3	4	5	6
d_i	-4.60	-3.40	2.25	3.75	4.33	2.80	3.87
Δ_i	-4.0	0.32	2.5	5.0	1.0	3.33	
α_i	0.25	0.25	0.25	0.25	0.25	0.25	
β_i	0.25	0.25	0.25	0.25	0.25	0.25	
γ_i	0.25	2.54	0.25	0.25	0.271	0.25	

B. NUMERICAL DEMONSTRATIONS

Example 1: In this subsection the numerical result for constrained data modeling is shown by using the data above y = 0.5x + 0.28 from Awang *et al.* [4] as shown in Table 1.

Figure 1(a) shows the example of constrained data modeling by using cubic spline interpolation. Clearly the curve in the second segment lies below the given straight line. To improve this, the proposed scheme is applied to the same data set. Figure 1(b) shows that, the proposed scheme produces the interpolating curve above the straight line.

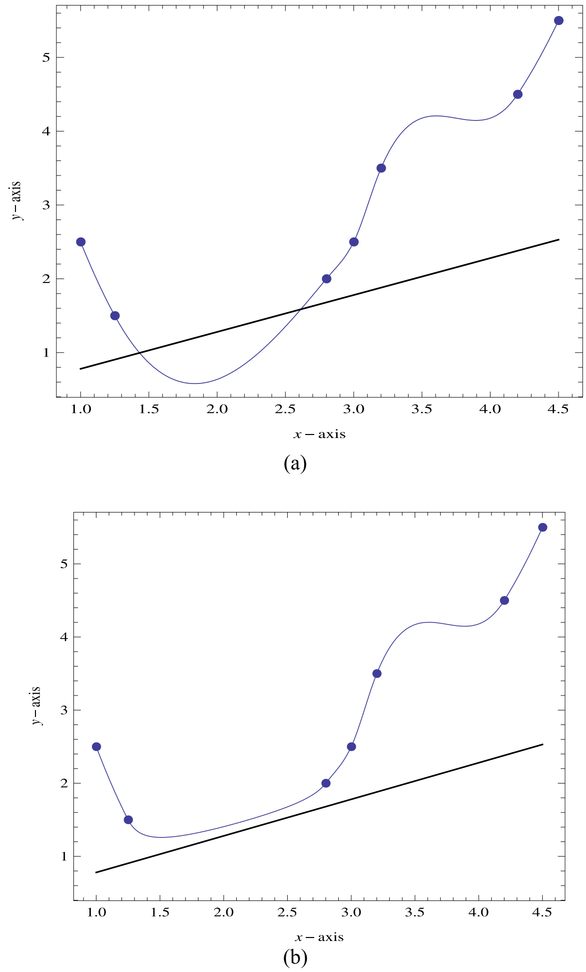

FIGURE 1. Comparison of (a) Cubic Hermite spline curve [14] (b) rational cubic spline with $\alpha_i = \beta_i = 0.25$.

C. RATIONAL BI-CUBIC SPLINE INTERPOLANT

The piecewise rational cubic spline in (1) can be extended to bi-cubic partially blended rational function $S(x, y)$ over rectangular meshes. The partially blended rational bi-cubic function over each rectangular patch $[x_i, x_{i+1}] \times [y_j, y_{j+1}]$, $i = 0, 1, \ldots, n-1; j = 0, 1, \ldots, m-1$ is defined as follows (Karim *et al.* [22]):

$$S(x, y) = -AFB^T, \quad (5)$$

where

$$F = \begin{pmatrix} 0 & S(x, y_j) & S(x, y_{j+1}) \\ S(x_i, y) & S(x_i, y_j) & S(x_i, y_{j+1}) \\ S(x_{i+1}, y) & S(x_{i+1}, y_j) & S(x_i, y_{j+1}) \end{pmatrix},$$

where

$$\begin{aligned} A &= \begin{bmatrix} -1 & a_0(\theta) & a_1(\theta) \end{bmatrix}, \\ B &= \begin{bmatrix} -1 & b_0(\phi) & b_1(\phi) \end{bmatrix}, \\ a_0(\theta) &= (1-\theta)^2(1+2\theta), \quad a_1(\theta) = \theta^2(3-2\theta), \\ b_0(\phi) &= (1-\phi)^2(1+2\phi), \quad b_1(\phi) = \phi^2(3-2\phi), \\ \theta &= \frac{x-x_i}{h_i}, \quad \phi = \frac{y-y_j}{\hat{h}_j}, \end{aligned}$$

and

$$h_i = x_{i+1} - x_i, \quad \hat{h}_j = y_{j+1} - y_j.$$

$S(x, y_j), S(x, y_{j+1}), S(x_i, y)$ and $S(x_{i+1}, y)$ are rational cubic function defined on the boundary of rectangular patch as follows: (see Figure 2 for illustration)

$$S(x, y_j) = \frac{\sum_{k=0}^{3}(1-\theta)^{3-k}\theta^k A_k}{q_1(\theta)}, \quad (6)$$

with

$$\begin{aligned} A_0 &= \alpha_{i,j}F_{i,j}, \\ A_1 &= \left(2\alpha_{i,j}\beta_{i,j} + \alpha_{i,j} + \gamma_{i,j}\right)F_{i,j} + \alpha_{i,j}h_iF^x_{i,j}, \\ A_2 &= \left(2\alpha_{i,j}\beta_{i,j} + \beta_{i,j} + \gamma_{i,j}\right)F_{i+1,j} - \beta_{i,j}h_iF^x_{i+1,j}, \\ A_3 &= \beta_{i,j}F_{i+1,j}, \\ q_1(\theta) &= (1-\theta)^2\alpha_{i,j} + \left(2\alpha_{i,j}\beta_{i,j} + \gamma_{i,j}\right) \\ &\quad \times \theta(1-\theta) + \theta^2\beta_{i,j}, \end{aligned}$$

$$S(x, y_{j+1}) = \frac{\sum_{k=0}^{3}(1-\theta)^{3-k}\theta^k B_k}{q_2(\theta)}, \quad (7)$$

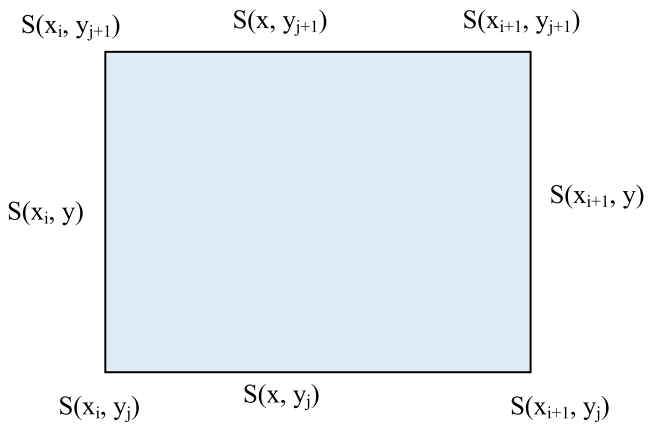

FIGURE 2. Rational Cubic Function Defined on Rectangular Patch Boundary.

with

$$\begin{aligned}
B_0 &= \alpha_{i,j+1}F_{i,j+1},\\
B_1 &= \left(2\alpha_{i,j+1}\beta_{i,j+1} + \alpha_{i,j+1} + \gamma_{i,j+1}\right)\\
&\quad \times F_{i,j+1} + \alpha_{i,j+1}h_iF^x_{i,j+1},\\
B_2 &= \left(2\alpha_{i,j+1}\beta_{i,j+1} + \beta_{i,j+1} + \gamma_{i,j+1}\right)\\
&\quad \times F_{i+1,j+1} - \beta_{i,j+1}h_iF^x_{i+1,j+1},\\
B_3 &= \beta_{i,j}F_{i+1,j+1},\\
q_2(\theta) &= (1-\theta)^2\alpha_{i,j+1} + \left(2\alpha_{i,j+1}\beta_{i,j+1} + \gamma_{i,j+1}\right)\\
&\quad \times \theta(1-\theta) + \theta^2\beta_{i,j+1},
\end{aligned}$$

$$S(x_i, y) = \frac{\sum_{k=0}^{3}(1-\phi)^{3-k}\phi^k C_k}{q_3(\phi)}, \tag{8}$$

with

$$\begin{aligned}
C_0 &= \hat{\alpha}_{i,j}F_{i,j},\\
C_1 &= \left(2\hat{\alpha}_{i,j}\hat{\beta}_{i,j} + \hat{\alpha}_{i,j} + \hat{\gamma}_{i,j}\right)F_{i,j} + \hat{\alpha}_{i,j}\hat{h}_jF^y_{i,j},\\
C_2 &= \left(2\hat{\alpha}_{i,j}\hat{\beta}_{i,j} + \hat{\beta}_{i,j} + \hat{\gamma}_{i,j}\right)F_{i,j+1} - \hat{\beta}_{i,j}\hat{h}_jF^y_{i,j+1},\\
C_3 &= \hat{\beta}_{i,j}F_{i,j+1},\\
q_3(\phi) &= (1-\phi)^2\hat{\alpha}_{i,j} + \left(2\hat{\alpha}_{i,j}\hat{\beta}_{i,j} + \hat{\gamma}_{i,j}\right)\\
&\quad \times \phi(1-\phi) + \phi^2\hat{\beta}_{i,j},
\end{aligned}$$

$$S(x_{i+1}, y) = \frac{\sum_{k=0}^{3}(1-\phi)^{3-k}\phi^k D_k}{q_4(\phi)}, \tag{9}$$

with

$$\begin{aligned}
D_0 &= \hat{\alpha}_{i+1,j}F_{i+1,j},\\
D_1 &= \left(2\hat{\alpha}_{i+1,j}\hat{\beta}_{i+1,j} + \hat{\alpha}_{i+1,j} + \hat{\gamma}_{i+1,j}\right)\\
&\quad \times F_{i+1,j} + \hat{\alpha}_{i+1,j}\hat{h}_jF^y_{i+1,j},\\
D_2 &= \left(2\hat{\alpha}_{i,+1j}\hat{\beta}_{i+1,j} + \hat{\beta}_{i+1,j} + \hat{\gamma}_{i+1,j}\right)\\
&\quad \times F_{i+1,j+1} - \hat{\beta}_{i+1,j}\hat{h}_jF^y_{i+1,j+1},\\
D_3 &= \hat{\beta}_{i,j}F_{i+1,j+1},\\
q_4(\phi) &= (1-\phi)^2\hat{\alpha}_{i+1,j} + \left(2\hat{\alpha}_{i+1,j}\hat{\beta}_{i+1,j} + \hat{\gamma}_{i+1,j}\right)\\
&\quad \times \phi(1-\phi) + \phi^2\hat{\beta}_{i+1,j}.
\end{aligned}$$

IV. RANGE RESTRICTED DATA INTERPOLATION

Common study in constraint surface interpolation or range restricted is that the construction of interpolating surface lies above a linear constraint plane. The problem statement for constrained surface interpolation to data above arbitrary plane can be described as follows:

Given the data, $\left(x_i, y_i, F_{i,j}\right), i = 0, 1, \ldots, n; j = 0, 1, \ldots, m$ defined over rectangular grid. $[x_i, x_{i+1}] \times \left[y_j, y_{j+1}\right], i = 0, 1, \ldots, n-1; j = 0, 1, \ldots, m-1$, the data lie above the plane

$$F_{i,j} > Z_{i,j}, \quad i = 0, 1, \ldots, n, \quad j = 0, 1, \ldots, m. \tag{10}$$

where $Z_{i,j} = Ax_i + By_j + C$, construct C^1 interpolating surface such that it will be lying above the given plane.

In this study we adopted the main idea in Chan and Ong [9] when deriving the sufficient conditions for constrained interpolation subject to a constraint plane up to degree three i.e. cubic plane. The derivation of condition is slightly different compared to the works of Abbas *et al.* [1], Hussain and Hussain [17], Hussain *et al.* [18] and Shaikh *et al.* [23]. The constraint plane $Z(x, y)$ can be considered as piecewise partially blended rational bi-cubic function. On each rectangle meshes, the four boundary curves of the constraint plane can be written as

$$Z\left(x, y_j\right) = \frac{\sum_{i=0}^{3}(1-\theta)^{3-i}\theta^i A_{1i}}{q_1(\theta)}, \tag{11}$$

with

$$\begin{aligned}
A_{10} &= \alpha_{i,j}Z_{i,j}\\
A_{11} &= \left(2\alpha_{i,j}\beta_{i,j} + \alpha_{i,j} + \gamma_{i,j}\right)Z_{i,j} + \alpha_{i,j}h_iZ^x_{i,j}\\
A_{12} &= \left(2\alpha_{i,j}\beta_{i,j} + \beta_{i,j} + \gamma_{i,j}\right)Z_{i+1,j} - \beta_{i,j}h_iZ^x_{i+1,j}\\
A_{13} &= \beta_{i,j}Z_{i+1,j}\\
q_1(\theta) &= (1-\theta)^2\alpha_{i,j} + \left(2\alpha_{i,j}\beta_{i,j} + \gamma_{i,j}\right)\\
&\quad \times \theta(1-\theta) + \theta^2\beta_{i,j};
\end{aligned}$$

$$Z\left(x, y_{j+1}\right) = \frac{\sum_{i=0}^{3}(1-\theta)^{3-i}\theta^i A_{2i}}{q_2(\theta)}, \tag{12}$$

with

$$\begin{aligned}
A_{20} &= \alpha_{i,j+1}Z_{i,j+1}\\
A_{21} &= \left(2\alpha_{i,j+1}\beta_{i,j+1} + \alpha_{i,j+1} + \gamma_{i,j+1}\right)\\
&\quad \times Z_{i,j+1} + \alpha_{i,j+1}h_iZ^x_{i,j+1}\\
A_{22} &= \left(2\alpha_{i,j+1}\beta_{i,j+1} + \beta_{i,j+1} + \gamma_{i,j+1}\right)\\
&\quad \times Z_{i+1,j+1} - \beta_{i,j+1}h_iZ^x_{i+1,j+1}\\
A_{23} &= \beta_{i,j}Z_{i+1,j+1}
\end{aligned}$$

$$q_2(\theta) = (1-\theta)^2\alpha_{i,j+1} + \left(2\alpha_{i,j+1}\beta_{i,j+1} + \gamma_{i,j+1}\right) \times \theta(1-\theta) + \theta^2\beta_{i,j+1}$$

$$Z(x_i, y) = \frac{\sum_{i=0}^{3}(1-\phi)^{3-i}\phi^i A_{3i}}{q_3(\phi)}, \quad (13)$$

with

$$\begin{aligned}
A_{30} &= \hat{\alpha}_{i,j}Z_{i,j}\\
A_{31} &= \left(2\hat{\alpha}_{i,j}\hat{\beta}_{i,j} + \hat{\alpha}_{i,j} + \hat{\gamma}_{i,j}\right)Z_{i,j} + \hat{\alpha}_{i,j}\hat{h}_jZ^y_{i,j}\\
A_{32} &= \left(2\hat{\alpha}_{i,j}\hat{\beta}_{i,j} + \hat{\beta}_{i,j} + \hat{\gamma}_{i,j}\right)Z_{i,j+1} - \hat{\beta}_{i,j}\hat{h}_jZ^y_{i,j+1}\\
A_{33} &= \hat{\beta}_{i,j}\, Z_{i,j+1}\\
q_3(\phi) &= (1-\phi)^2\hat{\alpha}_{i,j} + \left(2\hat{\alpha}_{i,j}\hat{\beta}_{i,j} + \hat{\gamma}_{i,j}\right) \times \phi(1-\phi) + \phi^2\hat{\beta}_{i,j};
\end{aligned}$$

$$Z(x_{i+1}, y) = \frac{\sum_{i=0}^{3}(1-\phi)^{3-i}\phi^i A_{4i}}{q_4(\phi)}, \quad (14)$$

with

$$\begin{aligned}
A_{40} &= \hat{\alpha}_{i+1,j}Z_{i+1,j}\\
A_{41} &= \left(2\hat{\alpha}_{i+1,j}\hat{\beta}_{i+1,j} + \hat{\alpha}_{i+1,j} + \hat{\gamma}_{i+1,j}\right) \times Z_{i+1,j} + \hat{\alpha}_{i+1,j}\hat{h}_jZ^y_{i+1,j}\\
A_{42} &= \left(2\hat{\alpha}_{i,+1j}\hat{\beta}_{i+1,j} + \hat{\beta}_{i+1,j} + \hat{\gamma}_{i+1,j}\right) \times Z_{i+1,j+1} - \hat{\beta}_{i+1,j}\hat{h}_jZ^y_{i+1,j+1}\\
A_{43} &= \hat{\beta}_{i,j}Z_{i+1,j+1}\\
q_4(\phi) &= (1-\phi)^2\hat{\alpha}_{i+1,j} + \left(2\hat{\alpha}_{i+1,j}\hat{\beta}_{i+1,j} + \hat{\gamma}_{i+1,j}\right) \times \phi(1-\phi) + \phi^2\hat{\beta}_{i+1,j}
\end{aligned}$$

where $Z^x_{i,j}$ and $Z^y_{i,j}$ indicate the partial derivatives of $Z(x, y)$ with respect to x and y at the node (x_i, y_j).

Let

$$G(x, y) = S(x, y) - Z(x, y) \quad (15)$$

then the constrained surface interpolation for surface $S(x, y)$ that lies above the given plane $Z(x, y)$ is reduced to the problem of positivity preserving interpolation for new surface $G(x, y)$ that satisfies the following conditions:

$$\begin{aligned}
G(x_i, y_j) &= F_{i,j} - Z_{i,j},\\
G^x(x_i, y_j) &= S^x(x, y) - Z^x(x, y) = F^x_{i,j} - Z^x_{i,j},\\
G^y(x_i, y_j) &= S^y(x, y) - Z^y(x, y) = F^y_{i,j} - Z^y_{i,j},\\
G^{xy}(x_i, y_j) &= S^{xy}(x, y) - Z^{xy}(x, y) = F^{xy}_{i,j} - Z^{xy}_{i,j}.
\end{aligned}$$

where $G^x(x_i, y_j)$, $G^y(x_i, y_j)$ and $G^{xy}(x_i, y_j)$ are partial derivatives at the respective knots. Similarly, for the partial derivatives of $S(x, y)$ and $Z(x, y)$.

The final interpolating surface $S(x, y)$ can be constructed by

$$S(x, y) = G(x, y) + Z(x, y).$$

Thus, the positivity preserving surface interpolation that has been developed in Karim *et al.* [22] can be used to construct the required positive interpolating surface $G(x, y)$. All four boundary curves can be written as follows:

$$G(x, y_j) = S(x, y_j) - Z(x, y_j) = \frac{\sum_{i=0}^{3}(1-\theta)^{3-i}\theta^i H_i}{q_1(\theta)} \quad (16)$$

with

$$\begin{aligned}
H_0 &= \alpha_{i,j}(F_{i,j} - Z_{i,j})\\
H_1 &= (2\alpha_{i,j}\beta_{i,j} + \alpha_{i,j} + \gamma_{i,j})(F_{i,j} - Z_{i,j}) + \alpha_{i,j}h_i\left(F^x_{i,j} - Z^x_{i,j}\right)\\
H_2 &= (2\alpha_{i,j}\beta_{i,j} + \beta_{i,j} + \gamma_{i,j})(F_{i+1,j} - Z_{i+1,j}) - \beta_{i,j}h_i\left(F^x_{i+1,j} - Z^x_{i+1,j}\right)\\
H_3 &= \beta_{i,j}(F_{i+1,j} - Z_{i+1,j});
\end{aligned}$$

$$G(x, y_{j+1}) = S(x, y_{j+1}) - Z(x, y_{j+1}) = \frac{\sum_{i=0}^{3}(1-\theta)^{3-i}\theta^i B_{1i}}{q_2(\theta)} \quad (17)$$

with

$$\begin{aligned}
B_{10} &= \alpha_{i,j+1}(F_{i,j+1} - Z_{i,j+1})\\
B_{11} &= (2\alpha_{i,j+1}\beta_{i,j+1} + \alpha_{i,j+1} + \gamma_{i,j+1}) \times (F_{i,j+1} - Z_{i,j+1}) + \alpha_{i,j+1}h_i\left(F^x_{i,j+1} - Z^x_{i,j+1}\right)\\
B_{12} &= (2\alpha_{i,j+1}\beta_{i,j+1} + \alpha_{i,j+1} + \gamma_{i,j+1}) \times (F_{i+1,j+1} - Z_{i+1,j+1}) - \beta_{i,j+1}h_i\left(F^x_{i+1,j+1} - Z^x_{i+1,j+1}\right)\\
B_{13} &= \beta_{i,j+1}(F_{i+1,j+1} - Z_{i+1,j+1});
\end{aligned}$$

$$G(x_i, y) = S(x_i, y) - Z(x_i, y) = \frac{\sum_{i=0}^{3}(1-\phi)^{3-i}\phi^i J_i}{q_3(\phi)} \quad (18)$$

with

$$\begin{aligned}
J_0 &= \hat{\alpha}_{i,j}(F_{i,j} - Z_{i,j})\\
J_1 &= \left(2\hat{\alpha}_{i,j}\hat{\beta}_{i,j} + \hat{\alpha}_{i,j} + \hat{\gamma}_{i,j}\right)(F_{i,j} - Z_{i,j}) + \hat{\alpha}_{i,j}\hat{h}_j\left(F^y_{i,j} - Z^y_{i,j}\right)\\
J_2 &= \left(2\hat{\alpha}_{i,j}\hat{\beta}_{i,j} + \hat{\beta}_{i,j} + \hat{\gamma}_{i,j}\right)(F_{i,j+1} - Z_{i,j+1}) - \hat{\beta}_{i,j}\hat{h}_j\left(F^y_{i,j+1} - Z^y_{i,j+1}\right)\\
J_3 &= \hat{\beta}_{i,j}(F_{i,j} - Z_{i,j+1});
\end{aligned}$$

$$G(x_{i+1}, y) = S(x_{i+1}, y) - Z(x_{i+1}, y) = \frac{\sum_{i=0}^{3} (1-\phi)^{3-i}\phi^i S_{1i}}{q_4(\phi)} \quad (19)$$

with

$$\begin{aligned} S_{10} &= \hat{\alpha}_{i+1,j}\left(F_{i+1,j} - Z_{i+1,j}\right) \\ S_{11} &= \left(2\hat{\alpha}_{i+1,j}\hat{\beta}_{i+1,j} + \hat{\alpha}_{i+1,j} + \hat{\gamma}_{i+1,j}\right) \\ &\quad \times \left(F_{i+1,j} - Z_{i+1,j}\right) \\ &\quad + \hat{\alpha}_{i+1,j}\hat{h}_j\left(F^y_{i+1,j} - Z^y_{i+1,j}\right) \\ S_{12} &= \left(2\hat{\alpha}_{i+1,j}\hat{\beta}_{i+1,j} + \hat{\beta}_{i+1,j} + \hat{\gamma}_{i+1,j}\right) \\ &\quad \times \left(F_{i+1,j+1} - Z_{i+1,j+1}\right) \\ &\quad - \hat{\beta}_{i+1,j}\hat{h}_j\left(F^y_{i+1,j+1} - Z^y_{i+1,j+1}\right) \\ S_{13} &= \hat{\beta}_{i+1,j}\left(F_{i+1,j+1} - Z_{i+1,j+1}\right). \end{aligned}$$

Thus, by using Theorem 2 in Karim *et al.* [22], the conditions for $G(x, y_j)$, $G(x, y_{j+1})$, $G(x_i, y)$ and $G(x_{i+1}, y)$ to be positive are

$$B_{1i} > 0, \quad H_i > 0, \quad J_i > 0, \quad S_{1i} > 0. \quad (20)$$

The results are stated in the following theorem.

Theorem 2: The piecewise partially blended rational bi-cubic function $S(x, y)$ in (1) defined over the rectangle $[x_i, x_{i+1}]\times[y_j, y_{j+1}]$, $i = 0, 1, \ldots, n-1; j = 0, 1, \ldots, m-1$, lying above the constraint plane $Z(x, y)$, if the parameters satisfy the following conditions:

$$\begin{aligned} &\alpha_{i,j} > 0, \quad \alpha_{i,j+1} > 0, \quad \beta_{i,j} > 0, \quad \beta_{i,j+1} > 0, \\ &\hat{\alpha}_{i,j} > 0, \quad \hat{\alpha}_{i+1,j} > 0, \quad \hat{\beta}_{i,j} > 0, \quad \hat{\beta}_{i+1,j} > 0, \\ \gamma_{i,j} &= \eta_{ij} + \text{Max}\{0, K_{10}, K_{11}\}, \\ \gamma_{i,j+1} &= \varepsilon_{ij} + \text{Max}\{0, K_{12}, K_{13}\}, \\ \hat{\gamma}_{i,j} &= \delta_{ij} + \text{Max}\{0, K_{14}, K_{15}\}, \\ \hat{\gamma}_{i+1,j} &= \chi_{ij} + \text{Max}\{0, K_{16}, K_{17}\}. \end{aligned} \quad (21)$$

with

$$K_{10} = -\alpha_{i,j}\left[\frac{h_i\left(F^x_{i,j} - Z^x_{i,j}\right)}{F_{i,j} - Z_{i,j}} + (2\beta_{i,j} + 1)\right],$$

$$K_{11} = \beta_{i,j}\left[\frac{h_i\left(F^x_{i+1,j} - Z^x_{i+1,j}\right)}{F_{i+1,j} - Z_{i+1,j}} - (2\alpha_{i,j} + 1)\right],$$

$$K_{12} = -\alpha_{i,j+1}\left[\frac{h_i\left(F^x_{i,j+1} - Z^x_{i,j+1}\right)}{F_{i,j+1} - Z_{i,j+1}} + (2\beta_{i,j+1} + 1)\right],$$

$$K_{13} = \beta_{i,j+1}\left[\frac{h_i\left(F^x_{i+1,j+1} - Z^x_{i+1,j+1}\right)}{F_{i+1,j+1} - Z_{i+1,j+1}} - (2\alpha_{i,j+1} + 1)\right],$$

$$K_{14} = -\hat{\alpha}_{i,j}\left[\frac{\hat{h}_j\left(F^y_{i,j} - Z^y_{i,j}\right)}{F_{i,j} - Z_{i,j}} + \left(2\hat{\beta}_{i,j} + 1\right)\right],$$

$$K_{15} = \hat{\beta}_{i,j}\left[\frac{\hat{h}_j\left(F^y_{i,j+1} - F^y_{i,j+1}\right)}{F_{i,j+1} - Z_{i,j+1}} - (2\hat{\alpha}_{i,j} + 1)\right],$$

$$K_{16} = -\hat{\alpha}_{i+1,j}\left[\frac{\hat{h}_j\left(F^y_{i+1,j} - Z^y_{i+1,j}\right)}{F_{i+1,j} - Z_{i+1,j}} + \left(2\hat{\beta}_{i+1,j} + 1\right)\right],$$

$$K_{17} = \hat{\beta}_{i+1,j}\left[\frac{\hat{h}_j\left(F^y_{i+1,j+1} - Z^y_{i+1,j+1}\right)}{F_{i+1,j+1} - Z_{i+1,j+1}} - (2\hat{\alpha}_{i+1,j} + 1)\right].$$

for $\eta_{i,j} > 0$, $\varepsilon_{i,j} > 0$, $\delta_{i,j} > 0$, $\chi_{i,j} > 0$.

Proof: We just show the proof for $G(x, y_j) > 0$. The other three boundary curves will follow similarly.

Now, $G(x, y_j) > 0$ if and only if $H_i > 0$, $i = 0, 1, 2, 3$. Clearly $H_0 > 0$ because $F_{i,j} - Z_{i,j} > 0$ and $H_3 > 0$ since $F_{i+1,j} - Z_{i+1,j} > 0$. Therefore, the sufficient condition for $G(x, y_j) > 0$ can be derived from inequalities:

$$H_1 > 0 \Rightarrow \left(2\alpha_{i,j}\beta_{i,j} + \alpha_{i,j} + \gamma_{i,j}\right)\left(F_{i,j} - Z_{i,j}\right) + \alpha_{i,j}h_i\left(F^x_{i,j} - Z^x_{i,j}\right) > 0$$

and

$$H_2 > 0 \Rightarrow \left(2\alpha_{i,j}\beta_{i,j} + \beta_{i,j} + \gamma_{i,j}\right)\left(F_{i+1,j} - Z_{i+1,j}\right) - \beta_{i,j}h_i\left(F^x_{i+1,j} - Z^x_{i+1,j}\right) > 0$$

Simplifies both inequalities lead us to:

$$\gamma_{i,j} > \text{Max}\{0, K_{10}, K_{11}\}$$

where

$$K_{10} = -\alpha_{i,j}\left[\frac{h_i\left(F^x_{i,j} - Z^x_{i,j}\right)}{F_{i,j} - Z_{i,j}} + (2\beta_{i,j} + 1)\right],$$

$$K_{11} = \beta_{i,j}\left[\frac{h_i\left(F^x_{i+1,j} - Z^x_{i+1,j}\right)}{F_{i+1,j} - Z_{i+1,j}} - (2\alpha_{i,j} + 1)\right].$$

which can be written as

$$\gamma_{i,j} = \eta_{ij} + \text{Max}\{0, K_{10}, K_{11}\}$$

for $\eta_{i,j} > 0$.

Similarly, we will obtain the remaining three conditions.

This completes the proof.

Algorithm I below can be used to construct the constrained interpolation for data lie above the given plane.

Remark 1: Case for constrained surface lie below arbitrary plane can be derived in the same manner as for above arbitrary plane. **Algorithm I** can be modified to accommodate for constrained surface lie below or between two planes.

V. NUMERICAL RESULTS

In this section, we test the capability of the proposed scheme by using five well-known data sets obtained from some established schemes as well as our own test function.

Algorithm 1 Construction of the Constrained Interpolation

Input: 3D data points $(x_i, y_j, F_{i,j})$, $i = 0, 1, \ldots, n$; $j = 0, 1, \ldots, m$ and the constraint plane $Z(x, y)$ such that $F_{i,j} > Z_{i,j}$.
Step 1: For $i = 0, 1, \ldots, n; j = 0, 1, \ldots, m$
Calculate the first derivative values $F^x_{i,j}$ and $F^y_{i,j}$ by using AMM and the first derivative values $Z^x_{i,j}$ and $Z^y_{i,j}$.
Step 2: For $i = 0, 1, \ldots, n-1; j = 0, 1, \ldots, m-1$
Choose suitable values for parameters $\alpha_{i,j}$, $\beta_{i,j}$, $\alpha_{i,j+1}$, $\beta_{i,j+1}$, $\hat{\alpha}_{i,j}$, $\hat{\alpha}_{i+1,j}$, $\hat{\beta}_{i,j}$, $\hat{\beta}_{i+1,j}$ and $\eta_{i,j}$, $\varepsilon_{i,j}$, $\delta_{i,j}$, $\chi_{i,j}$. Compute the values of parameters $\gamma_{i,j}$, $\gamma_{i,j+1}$, $\hat{\gamma}_{i,j}$, $\hat{\gamma}_{i+1,j}$ by using Condition (21).
Step 3: Construct the constrained interpolating surface lies above the plane $Z(x, y)$ by substituting all the required parameters into the partially blended rational bi-cubic spline function defined by (5).
Output: Constrained interpolating surface lying above the constraint plane

TABLE 3. Constrained surface data from function $F(x, y)$.

y/x	1	2	3	4	5	6
1	1.6456	0.8498	0.3670	0.6500	1.4387	2.008
2	1.6913	0.8216	0.2998	0.6056	1.4579	2.0731
3	1.2762	1.1413	1.0603	1.1078	1.2400	1.3355
4	0.7911	1.5149	1.9492	1.6947	0.9853	0.4733
5	0.6819	1.5991	2.1493	1.8268	0.9280	0.2793
6	1.0490	1.3163	1.4766	1.3826	1.1207	0.9317

TABLE 4. Data from plane $Z = 1 - \frac{x}{6} - \frac{y}{6}, 1 \leq x, y \leq 6$.

y/x	1	2	3	4	5	6
1	0.6667	0.5	0.3333	0.1667	0	-0.1667
2	0.5000	0.3333	0.1667	0	-0.1667	-0.3333
3	0.3333	0.1667	0	-0.1667	-0.3333	-0.5
4	0.1667	0	-0.1667	-0.3333	-0.5	-0.6667
5	0	-0.1667	-0.3333	-0.5	-0.6667	-0.8333
6	-0.1667	-0.3333	-0.5	-0.6667	-0.8333	-1

In Examples 2 and 3, we consider the data that lies above a linear plane. Meanwhile in Examples 4 and 5, we consider when the data lie above quadratic and cubic planes, respectively. Finally, in Example 6, we implement the proposed scheme for the data lie between two planes. MATLAB 2015 version installed on Intel® Core ™ i5-3470 3.20GHz is used to produce all graphical and numerical results.

Example 2: A constrained data points from the following function is truncated to four decimal places [1].

$$F(x, y) = \sin(x)\cos(y) + 1.2, \quad 1 \leq x, \quad y \leq 6 \tag{22}$$

Figure 3 shows the true surface of function $F(x, y)$ which is above the constraint plane $Z = 1 - \frac{x}{6} - \frac{y}{6}$.

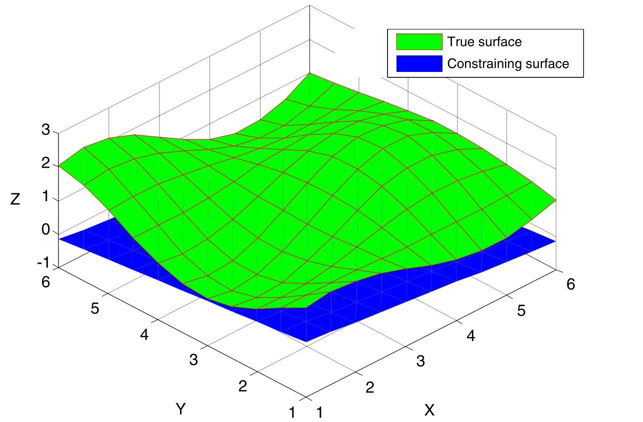

FIGURE 3. True function $F(x, y)$ and constraining surface.

TABLE 5. Constrained surface data from function $F_2(x, y)$.

y/x	1	2	3	4	5	6
1	3.8189	3.245	2.2886	2.2886	3.245	2.8513
2	3.0507	2.4768	1.5204	1.5204	2.4768	3.0507
3	3.1185	2.5447	1.5882	1.5882	2.5447	3.1185
4	4.8015	4.2276	3.2712	3.2712	4.2276	4.8015
5	4.8693	4.2954	3.339	3.339	4.2954	4.8693
6	4.1011	3.5273	2.5708	2.5708	3.5273	4.1011

The default of bi-cubic Hermite spline is shown in Figure 4(a). Figure 4(b) shows the *xz*-view and Figure 4(c) shows the other view for Figure 4(a) respectively. Figure 4(c) clearly show that the interpolating surface lies below the plane. This flaw is recovered nicely by using the proposed scheme in this study as shown in Figure 5. Figure 5(a) shows the constrained data modeling by using the proposed rational bi-cubic spline with $\alpha_{i,j} = \beta_{i,j} = 1.5$, $\hat{\alpha}_{i,j} = \hat{\beta}_{i,j} = 1.5$,while Figure 5(b) shows the *xz*-view for Figure 5(a) respectively. Figure 5(c) shows that the resulting interpolating surface by using Abbas *et al.* [1] scheme. Furthermore, the absolute error surface of function $F(x, y)$ by using the proposed method is shown in Figure 6.

Example 3: A constrained data points from the following function is truncated to four decimal places ([1]).

$$F_2(x, y) = \sin(x) - \cos(y) + 2.97, \tag{23}$$

Figure 7 shows the true surface of function F_2 which is above the constraint plane $Z = 1 - \frac{x}{6} - \frac{y}{6}, -3 \leq x, y \leq 3$. Figure 8(a) shows the default bi-cubic Hermite spline for the constrained data given in Table 5.

Figure 8(b) shows the *xz*-view and Figures 8(c) and 8(d) show the other view for Figure 8(a) respectively. Some part of the interpolating surface lies below the given plane as shown in Figure 8(d).

Figure 9 shows the constrained data modeling by using the proposed rational bi-cubic spline with $\alpha_{i,j} = \beta_{i,j} = 1.5$,

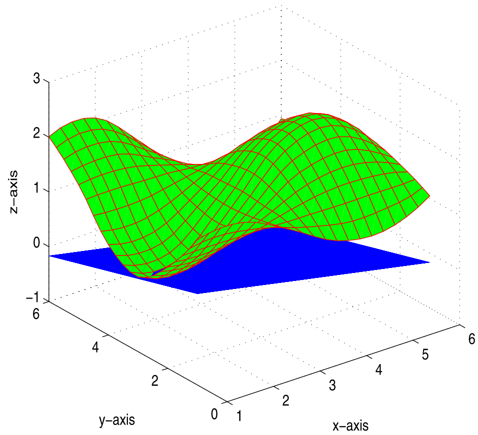

(a) Bi-cubic Hermite

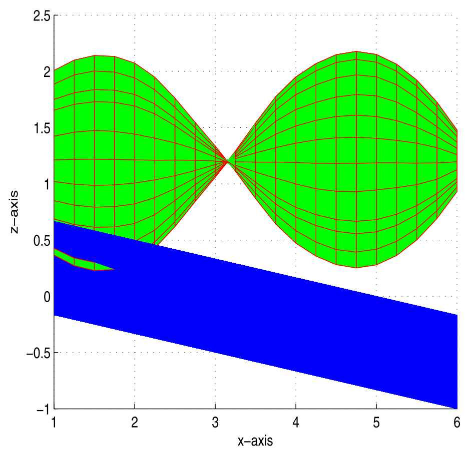

(b) xz -view of Figure 4(a)

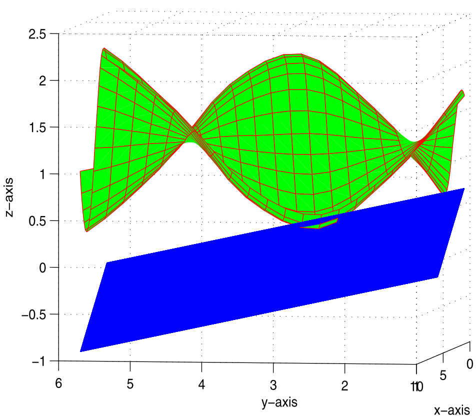

(c) Other view for Figure 4(a)

FIGURE 4. Bi-cubic Hermite surface.

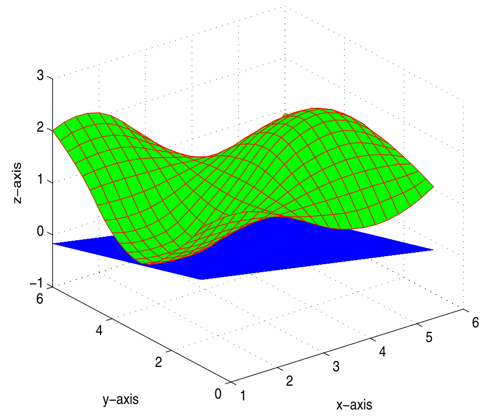

(a) Constrained surface using the proposed scheme

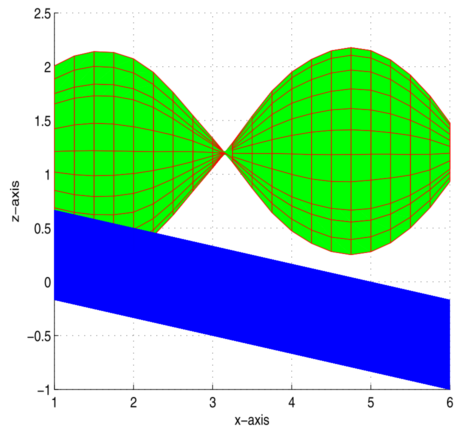

(b) xz -view of Figure 5(a)

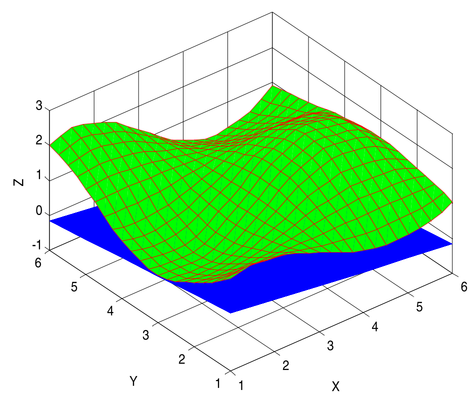

(c) Constrained surface from Abbas et al. [1]

FIGURE 5. Interpolating surfaces for Example 2.

$\hat{\alpha}_{i,j} = \hat{\beta}_{i,j} = 1.5$. Meanwhile Figure 9(b) and 9(c) show the xz-view and other view for Figure 9(a) respectively. Figure 9(d) shows that the resulting interpolating surfaces lying above the given plane. Finally Figure 9(e) shows the surface by using Abbas *et al.* [1] scheme. Both schemes are capable to preserves the shape of the data. Figure 10 shows the absolute error surface of function F_2 by using the proposed method.

Example 4: The following example consider the constrained data points from surface $F_3(x, y)$and lies above the quadratic plane $Z(x, y)$ given in Equations (24) and (25)

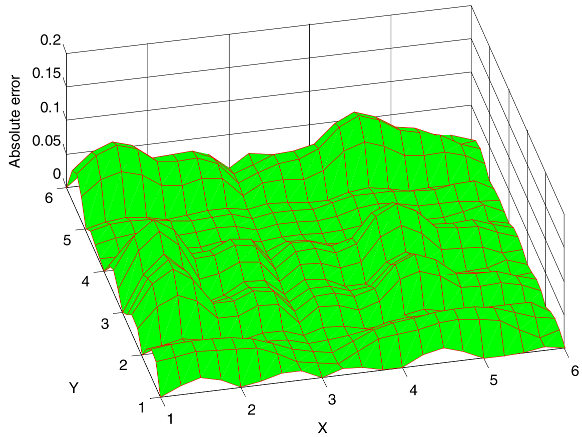

FIGURE 6. **Error surface of $F(x, y)$ using the proposed scheme.**

TABLE 6. **Data from plane $Z = 1 - \frac{x}{6} - \frac{y}{6}, -3 \leq x, y \leq 3$.**

y/x	-3	-2	-1	1	2	3
-3	2	1.8333	1.6667	1.3333	1.1667	1
-2	1.8333	1.6667	1.5	1.1667	1	0.8333
-1	1.6667	1.5	1.3333	1	0.8333	0.6667
1	1.3333	1.1667	1	0.6667	0.5	0.3333
2	1.1667	1	0.8333	0.5	0.3333	0.1667
3	1	0.8333	0.6667	0.3333	0.1667	0

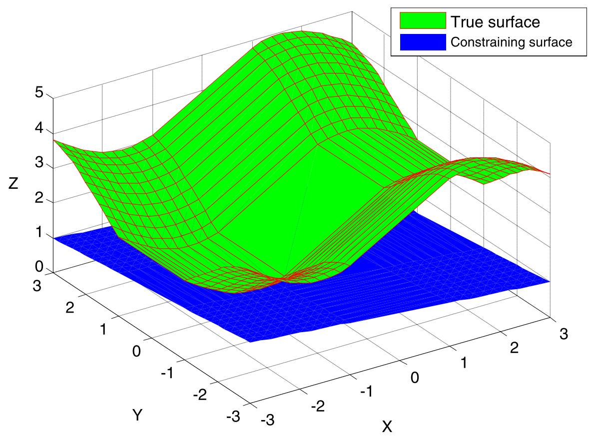

FIGURE 7. **True function $F_2(x, y)$ and constraining surface.**

respectively.

$$F_3(x, y) = \sin(x)\cos(x) + 0.35, \quad -3 \leq x, \quad y \leq 3 \tag{24}$$

$$Z(x, y) = -0.55x^2 - 1.35x - 0.2xy - 0.2y - 1.39 \tag{25}$$

The first partial derivative for the quadratic plane $Z(x, y)$ are calculated analytically from the original plane. For instance

$$Z_x(x, y) = -1.1x - 1.35 - 0.2x$$

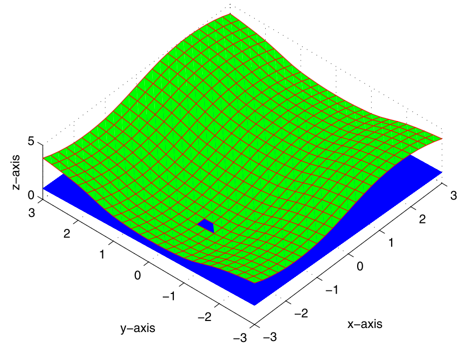

(a) Bi-cubic Hermite surface

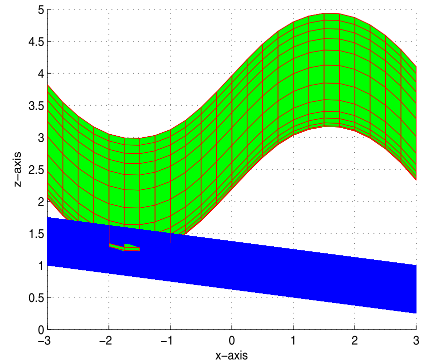

(b) xz -view of Figure 8(a)

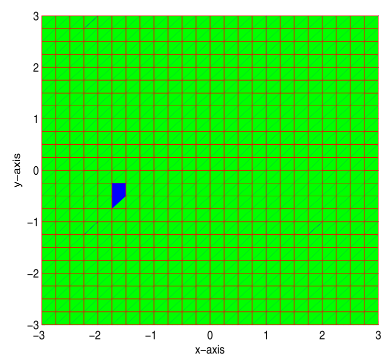

(c) Other view of Figure 8(a)

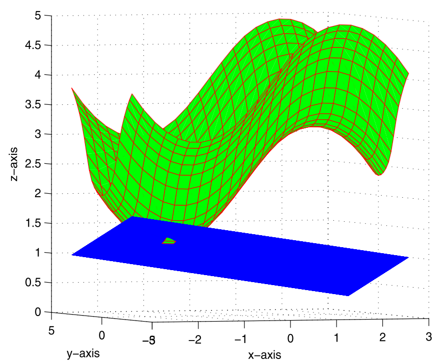

(d) Other view of Figure 8(a)

FIGURE 8. **Bi-cubic Hermite Surface.**

and

$$Z_y(x, y) = 0.2x - 0.2$$

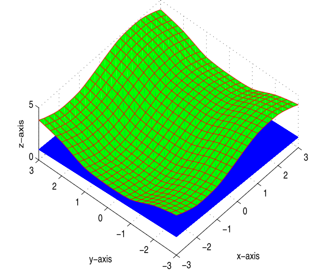

(a) Constrained surface using the proposed scheme

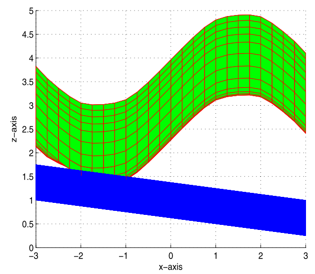

(b) xz -view of Figure 9(a)

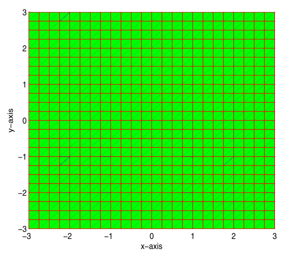

(c) Other view of Figure 9(a)

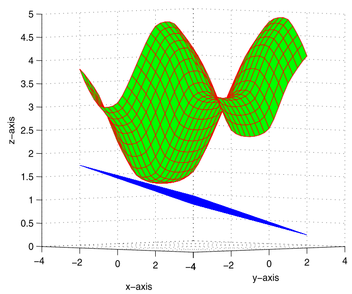

(d) Other view of Figure 9(a)

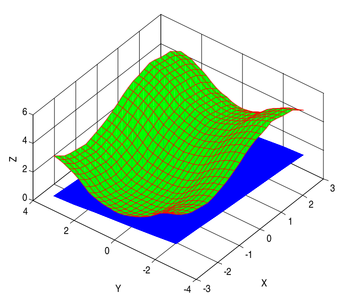

(e) Abbas et al. [1] scheme

FIGURE 9. Interpolating surfaces for Example 3.

Figure 11 shows the true surface of function F_3 which is above the constrained plane

$$Z(x, y) = -0.55x^2 - 1.35x - 0.2xy - 0.2y - 1.39$$

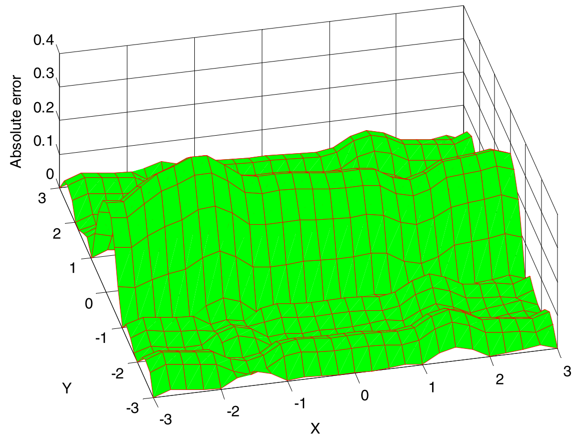

FIGURE 10. Error surface of F_2 using the proposed scheme.

TABLE 7. Constrained surface data from function $F_3(x, y)$.

y/x	-3	-2	-1	0	1	2	3
-3	0.4897	1.2502	1.1830	0.35	-0.4830	-0.5502	0.2103
-2	0.4087	0.7284	0.7002	0.35	-0.0002	-0.0284	0.2913
-1	0.2738	-0.1413	-0.1046	0.35	0.8046	0.8413	0.4262
0	0.2089	-0.5593	-0.4915	0.35	1.1915	1.2593	0.4911
1	0.2738	-0.1413	-0.1046	0.35	0.8046	0.8413	0.4262
2	0.4087	0.7284	0.7002	0.35	-0.0002	-0.0284	0.2913
3	0.4897	1.2502	1.1830	0.35	-0.4830	-0.5502	0.2103

TABLE 8. Data from plane $Z(x, y) = -0.55x^2 - 1.35x - 0.2xy - 0.2y - 1.39$.

y/x	-3	-2	-1	0	1	2	3
3	-3.49	-1.49	-0.59	-0.79	-2.09	-4.49	-7.99
-2	-3.09	-1.29	-0.59	-0.99	-2.49	-5.09	-8.79
-1	-2.69	-1.09	-0.59	-1.19	-2.89	-5.69	-9.59
0	-2.29	-0.89	-0.59	-1.39	-3.29	-6.29	-10.39
1	-1.89	-0.69	-0.59	-1.59	-3.69	-6.89	-11.19
2	-1.49	-0.49	-0.59	-1.79	-4.09	-7.49	-11.99
3	-1.09	-0.29	-0.59	-1.99	-4.49	-8.09	-12.79

Figure 12 (a) shows the default bi-cubic Hermite spline for the constrained data given in Table 7.

Figure 12(b) shows the xz-view for Figure 12(a). From the figures, some part of the interpolating surface through bi-cubic Hermite lying below the given plane. Figure 13(a) shows the constrained data modeling by using the proposed rational bi-cubic spline with, while Figure 13(b) shows the xz-view for Figure 13(a). Figure 13(a) and 13(b) show that the resulting interpolating surfaces lying above the given plane. Figure 14 shows the absolute error surface of function F_3 by using the proposed scheme in this study.

Example 5: Our next example consider the constrained data points from surface $F_4(x, y)$ and lies above the cubic

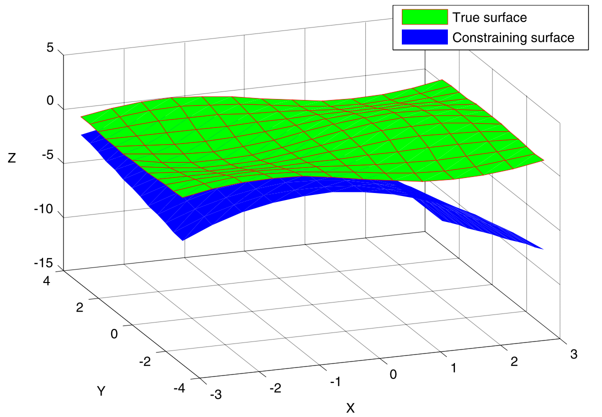

FIGURE 11. **True surface $F_3(x, y)$ and constraining surface.**

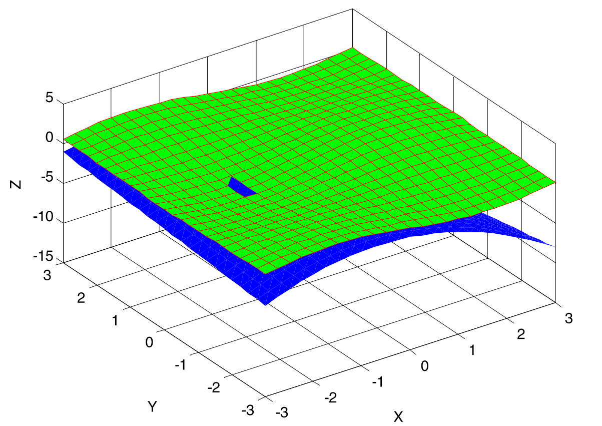

(a) Bicubic Hermite Surface

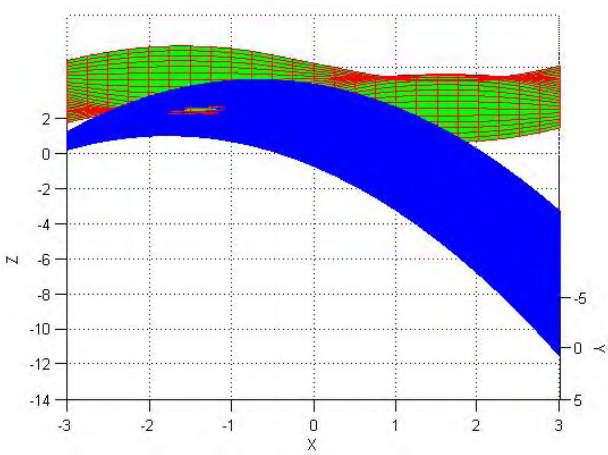

(b) xz view of 11 (a)

FIGURE 12. **Bi-cubic Hermite Surface.**

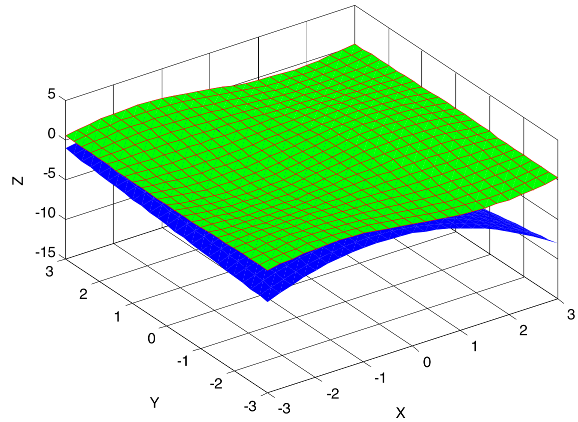

(a) Constrained surface using the proposed scheme

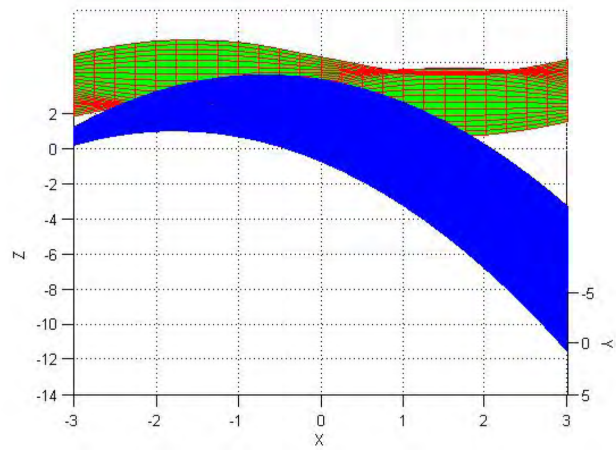

(b) xz view of 12(a)

FIGURE 13. **Interpolating surfaces for Example 4.**

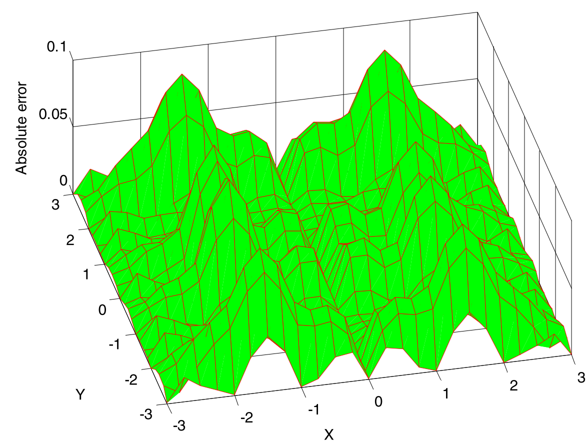

FIGURE 14. **Error surface of F_3 using the propose scheme.**

planeZ (x, y) given in Equations (26) and (28) respectively.

$$F_4(x,y) = 1.025 - 0.75e^{\left(-(6x-1)^2+(6y-1)^2\right)} + 0.5e^{\left(-(10x-4)^2-(10y-7)^2\right)} \quad (26)$$

$$- 0.5e^{\left(-(9x-7)^2+(9y-3)^2/4\right)} - 0.75e^{\left(-(9x+1)^2/49-(9y+1)/10\right)} \quad (27)$$

$$Z(x,y) = 3x^3 + 5.5x + 0.2xy - 2.25y + 0.08 \quad (28)$$

Figure 15 shows the true surface of function F_4 which is above the cubic constraint surface.

$$Z(x,y) = 3x^3 + 5.5x + 0.2xy - 2.25y + 0.08.$$

TABLE 9. Constrained surface data from function $F_4(x, y)$.

y/x	0	0.2	0.4	0.6	0.8	1.0
0	0.2586	0.1816	0.5426	0.7027	0.8008	0.9174
0.2	0.2045	0.1508	0.5361	0.5945	0.5359	0.8230
0.4	0.5222	0.5195	0.6772	0.5787	0.4525	0.7954
0.6	0.6372	0.6837	0.5776	0.7877	0.8074	0.9300
0.8	0.7013	0.7401	0.6262	0.8752	0.9352	0.9798
1.0	0.7547	0.7899	0.8458	0.9054	0.9550	0.9891

TABLE 10. Data from plane $Z(x, y) = 3x^3 + 5.5x + 0.2xy - 2.25y + 0.08$.

x/y	0	0.2	0.4	0.6	0.8	1.0
0	0.08	-0.174	-0.132	0.062	0.2640	0.3300
0.2	0.08	-0.166	-0.116	0.086	0.2960	0.3700
0.4	0.08	-0.158	-0.100	0.110	0.3280	0.4100
0.6	0.08	-0.150	-0.084	0.134	0.3600	0.4500
0.8	0.08	-0.142	-0.068	0.158	0.3920	0.4900
1.0	0.08	-0.134	-0.052	0.182	0.4240	0.5300

TABLE 11. Data for example 6.

x/y	0.0	0.25	0.5	0.75	1.0
0.0	0.0	0.5	1.0	1.0	1.0
0.5	0.0	0.0	0.0	0.5	1.0
1.0	0.0	0.0	0.0	0.0	0.0
1.5	0.0	0.0	1.0	0.0	0.0
2.0	0.0	0.0	0.0	0.0	0.0

Figure 16(a) shows the default bi-cubic Hermite spline the constrained data given in Table 9. Figure 16(b) shows the xz-view for Figure 16(a). Some part of the interpolating surface through bi-cubic Hermite lying below the given plane as shown in Figure 16(b). Figure 17(a) shows the constrained data modeling by using the proposed rational bi-cubic spline, while Figure 17(b) shows the xz-view of Figure 17(a). Clearly seen, the resulting interpolating surface lie above the given cubic plane. Figure 18 shows the absolute error surface of function F_4 by using the proposed scheme.

Example 6: Our final example considers the following function

$$F_5(x, y) = \begin{cases} 1.0, & \text{if } (y - x) \geq 0.5 \\ 2(y - x), & \text{if } 0 \leq (y - x) \leq 0.5 \\ \dfrac{\cos\left(4\pi\sqrt{(x-1.5)^2 + (y-0.5)^2}\right) + 1}{2} & \text{if } (x-1.5)^2 + (y-0.5)^2 \\ 0 & \text{elsewhere on } [0, 2] \times [0, 2] \end{cases}$$

the constant plane chosen as follows:

Upper Plane: z = 1

Lower Plane: z = 0

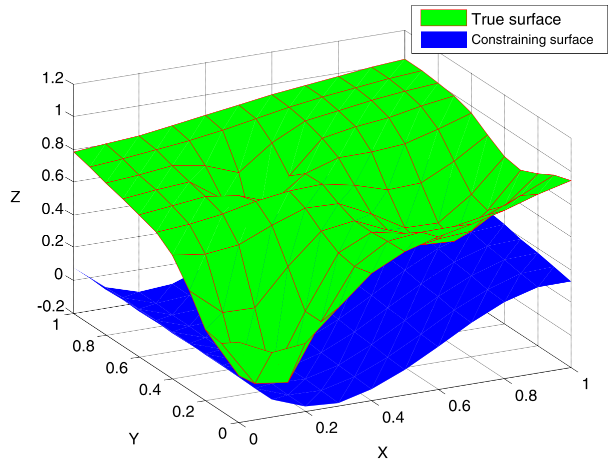

FIGURE 15. True surface $F_4(x, y)$ and constraining surface.

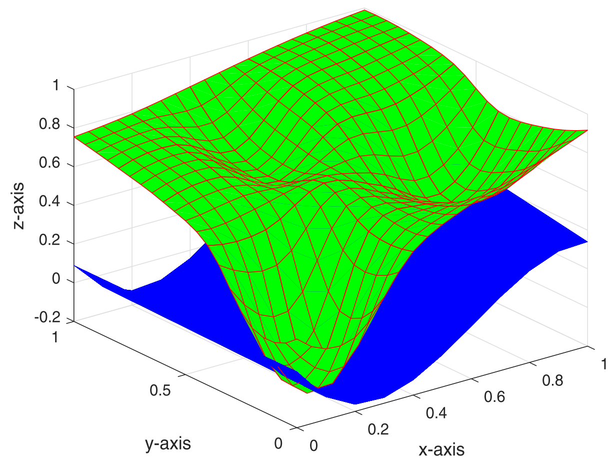

(a) Bicubic Hermite Surface

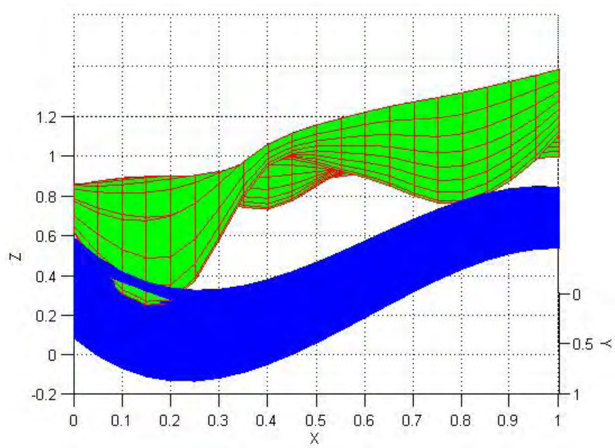

(b) xz -view of (a)

FIGURE 16. Bi-cubic Hermite Surface. (a) Bicubic Hermite Surface. (b) xz-view of (a).

Figure 19 shows the examples of constrained surface produced by bi-cubic Hermite surface as well as the proposed scheme. Meanwhile, Figure 20 shows the constrained

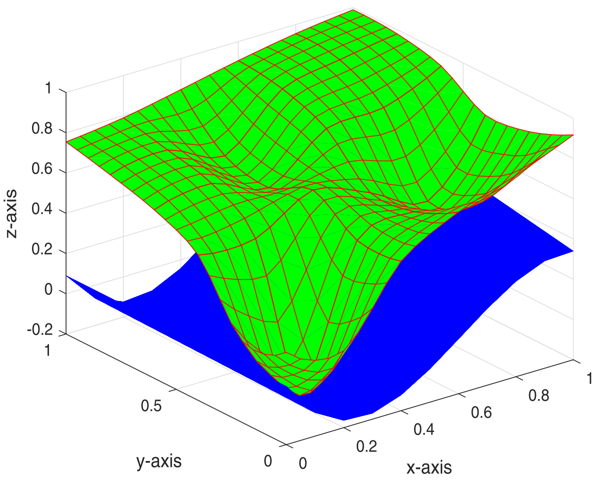

(a) Constrained surface using the proposed scheme

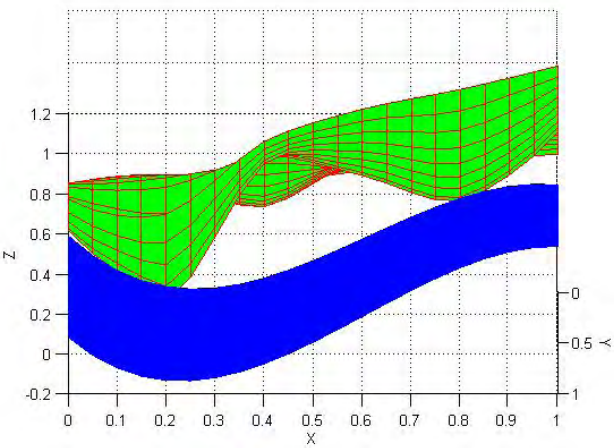

(b) xz -view of 16(a)

FIGURE 17. Interpolating surfaces for Example 4.

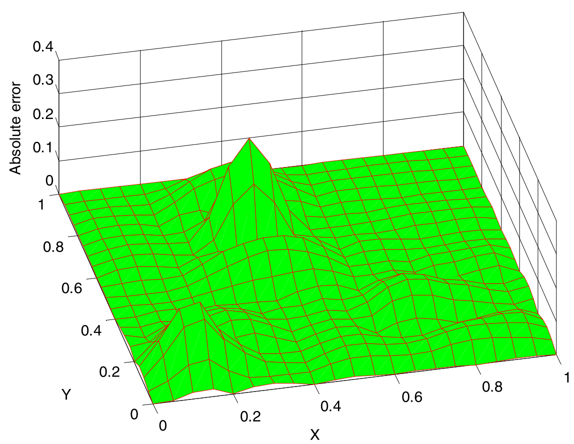

FIGURE 18. Error surface of F_4 using the propose scheme.

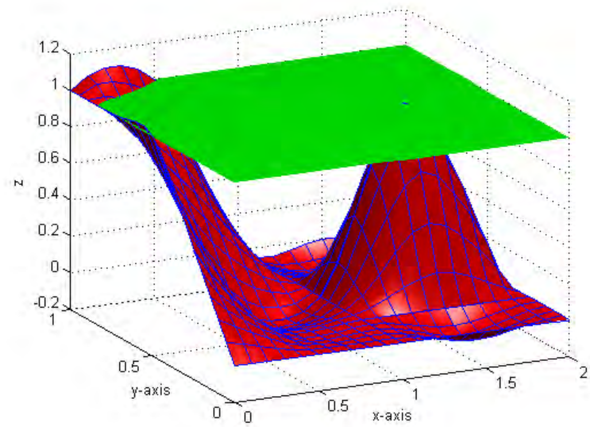

(a) Bicubic hermite surface

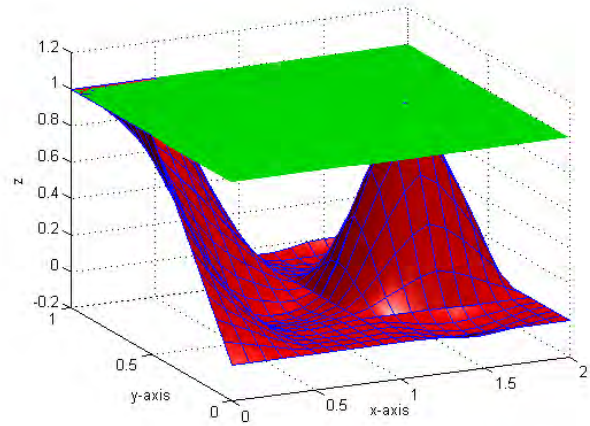

(b) Constrained surface using the proposed scheme

FIGURE 19. Constrained surface below the plane.

surface between two planes produced by using bi-cubic Hermite and the constructed rational bi-cubic spline. From Figures 20(a) and 20(a), clearly seen that, bi-cubic Hermite surface is unable to produce constrained surface. But by using the proposed scheme in this study, the produced surface satisfies the range restricted shape preserving properties. Figure 20(b) shows that, we obtain surface lie between two planes.

To measure the effectiveness of the proposed scheme, we calculate R^2, RMSE and CPU Times in seconds. Table 12 shows the error estimation between the proposed scheme and Abbas *et al.* [1] scheme.

Based on the result from Table 12, for the constrained interpolation in Example 2 and Example 3, the proposed scheme is better than Abbas *et al.* [1] scheme in the sense of CPU times measured in seconds. For both examples, the proposed scheme requires less computation time than Abbas *et al.* [1]. In terms of R^2 and RMSE, for Example 2, the proposed scheme is better. But for Example 3, Abbas *et al.* [1] scheme has lower RMSE i.e. 0.0093 while the proposed scheme has the value 0.0145. But from the Figures, based on graphical displays, both schemes produce equally visually pleasant interpolating surface. For Examples 4 and 5,

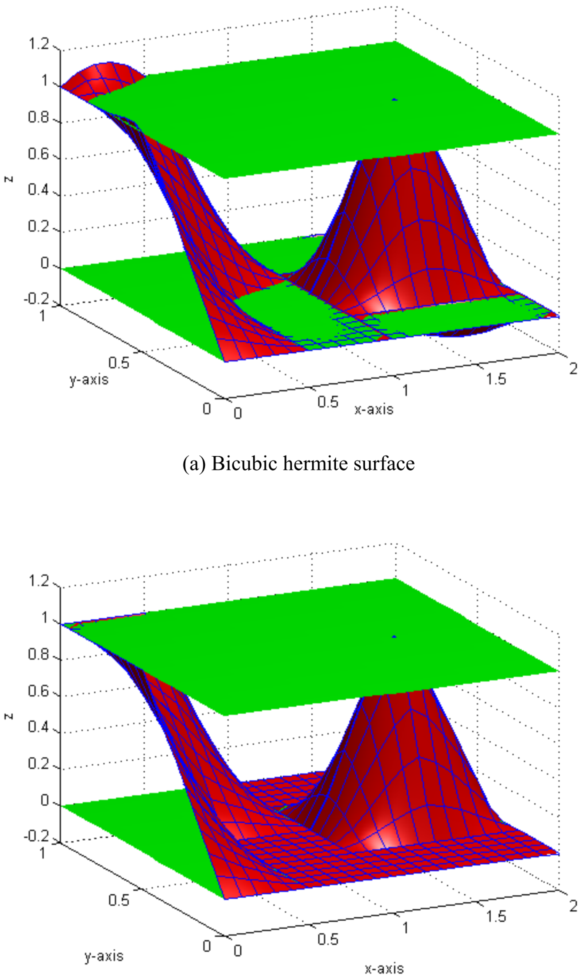

(a) Bicubic hermite surface

(b) Constrained surface using the proposed scheme

FIGURE 20. **Constrained surface between two planes.**

TABLE 12. **Error estimation.**

Method	Measure -ment	Data Sets			
		Example 2	Example 3	Example 4	Example 5
Abbas et al. [1]	R^2	0.9941	0.9902	N/A	N/A
	RMSE	0.0015	0.0093	N/A	N/A
	CPU Times (s)	2.5871	3.2962	N/A	N/A
The proposed scheme	R^2	0.9954	0.9846	0.9861	0.9701
	RMSE	0.0011	0.0145	0.0035	0.0018
	CPU Times (s)	1.1935	2.3603	2.20460	2.79974

Abbas *et al.* [1] is not be implemented. This is due to the fact that their scheme is only capable to construct constrained surface above linear plane only. We implement the proposed scheme in this study for the constraint surfaces are quadratic and cubic planes, respectively. From the results, we found that, the proposed scheme has the ability to preserve the shape of the data and better than Abbas *et al.* [1] in terms of CPU time, RMSE and R^2. Furthermore, we also tested the proposed scheme for constrained surface interpolation subject to range restricted below plane and between two planes. Figures 18 and 19 shows the results. Numerical results also show that, the proposed scheme give higher accuracy with higher R^2 value i.e. **between 0.9701 (97.01%) and 0.9954 (99.54%).** This is very good for constraint surface or range restricted data interpolation.

VI. CONCLUSIONS

This paper discusses the application of partially blended rational bi-cubic spline with twelve parameters on rectangular meshes for constrained data modeling. The sufficient conditions are derived on four parameters meanwhile the remaining eight parameters can be further utilized to obtain the desired constrained interpolating surfaces. The resulting surface is guaranteed has C^1 continuity by extending the main result from Casciola and Romani [8]. From numerical results and the comparison with existing schemes we conclude that the proposed schemes work very well and it is easy to use, require less computation compared to the work of Hussain *et al.* [17] and Abbas *et al.* [1]. Furthermore, the proposed scheme has eight free parameters while there are no free parameters in the works of Hussain *et al.* [18], Hussain *et al.* [19], and Shaikh *et al.* [21]. We also have considered the constrained interpolation above quadratic and cubic plane, meanwhile in the works of Hussain and Hussain [18], Abbas *et al.* [1], Shaikh *et al.* [21] and Hussain and Hussain [17], they only consider the constrained interpolation above linear plane. Thus, the results presented in this study is more generalize than those mentioned schemes. Furthermore, for all examples, the proposed scheme gives very higher R^2 value. Based on all measurements and validation, we conclude that the proposed scheme is better than some existing scheme. The main future work will be on applying the proposed schemes for industrial based applications such as in robotics and manufacturing as well as in medical image processing, for instance image refinement and image scaling.

REFERENCES

[1] M. Abbas, A. A. Majid, and J. M. Ali, "Constrained shape preserving rational bi-cubic spline interpolation," *World Appl. Sci. J.*, vol. 20, no. 6, pp. 790–800, 2012.

[2] M. R. Asim and K. W. Brodlie, "Curve drawing subject to positivity and more general constraints," *Comput. Graph.*, vol. 27, pp. 469–485, Aug. 2003.

[3] M. R. Asim, G. Mustafa, and K. W. Brodlie, "Constrained visualization of 2D positive data using modified quadratic Shepard method," in *Proc. MSCG POSTERS WSCG*, Plzen, Czech Republic, Feb. 2004, pp. 1–6.

[4] M. N. Awang, M. Abbas, A. A. Majid, and J. M. Ali, "Data visualization for constrained data using rational cubic spline," in *Proc. World Congr. Eng. Comput. Sci. (WCECS)*, San Francisco, CA, USA, vol. 1, Oct. 2013, pp. 80–85.

[5] K. W. Brodlie, P. Mashwama, and S. Butt, "Visualization of surface data to preserve positivity and other simple constraints," *Comput. Graph.*, vol. 19, no. 4, pp. 585–594, 1995.

[6] K. W. Brodlie, M. R. Asim, and K. Unsworth, "Constrained visualization using the shepard interpolation family," *Comput. Graph. Forum*, vol. 24, no. 4, pp. 809–820, 2005.

[7] S. Butt and K. W. Brodlie, "Preserving positivity using piecewise cubic interpolation," *Comput. Graph.*, vol. 17, no. 1, pp. 55–64, 1993.

[8] G. Casciola and L. Romani, "Rational interpolants with tension parameters," in *Curve and Surface Design*, T. Lyche, M.-L. Mazure, and L. L. Schumaker, Eds. Brentwood, U.K.: Nashboro Press, 2003, pp. 41–50.

[9] E. S. Chan and B. H. Ong, "Range restricted scattered data interpolation using convex combination of cubic Bézier triangles," *J. Comput. Appl. Math.*, vol. 136, pp. 135–147, Nov. 2001.

[10] P. Constantini and F. Fontanella, "Shape-preserving bivariate interpolation," *SIAM J. Numer. Anal.*, vol. 27, no. 2, pp. 488–506, 1990.

[11] Q. Duan, K. Djidjeli, W. G. Price, and E. H. Twizell, "Constrained control and approximation properties of a rational interpolating curve," *Inf. Sci.*, vol. 152, pp. 181–194, Jun. 2003.

[12] Q. Duan, X. Wang, and F. Cheng, "Constrained interpolation using rational cubic spline with linear denominators," *Korean J. Comput. Appl. Math.*, vol. 1, pp. 203–215, Jan. 1999.

[13] Q. Duan, H. Zhang, Y. Zhang, and E. H. Twizell, "Error estimation of a kind of rational spline," *J. Comput. Appl. Math.*, vol. 200, pp. 1–11, Mar. 2007.

[14] G. E. Farin, *Curves and Surfaces for CAGD: A Practical Guide*, 5th ed. San Mateo, CA, USA: Morgan Kaufmann, 2002.

[15] T. N. T. Goodman, B. H. Ong, and K. Unsworth, "Constrained interpolation using rational cubic splines," in *NURBS for Curve and Surface Design*, G. Farin, Ed. Philadelphia, PA, USA: SIAM, 1991, pp. 59–74.

[16] M. Z. Hussain and M. Sarfraz, "Positivity-preserving interpolation of positive data by rational cubics," *J. Comput. Appl. Math.*, vol. 218, no. 2, pp. 446–458, 2008.

[17] M. Z. Hussain and M. Hussain, "Visualization of data subject to positive constraint," *J. Inf. Comput. Sci.*, vol. 1, no. 3, pp. 149–160, 2006.

[18] M. Z. Hussain, M. Sarfraz, and M. Hussain, "Visualization of constrained data by rational cubics," *Eur. J. Sci. Res.*, vol. 21, no. 1, pp. 212–228, 2008.

[19] M. Z. Hussain, M. Sarfraz, and A. Shakeel, "Shape preserving surfaces for the visualization of positive and convex data using rational bi-quadratic splines," *Int. J. Comput. Appl.*, vol. 27, no. 10, pp. 12–20, 2011.

[20] F. Ibraheem, M. Hussain, M. Z. Hussain, and A. A. Bhatti, "Monotone data visualization using rational trigonometric spline interpolation," *Sci. World J.*, vol. 2014, Apr. 2014, Art. no. 602453.

[21] S. A. A. Karim and V. P. Kong, "Shape preserving interpolation using rational cubic spline," *Res. J. Appl. Sci., Eng. Technol.*, vol. 8, no. 2, pp. 167–168, 2014.

[22] S. A. A. Karim, V. P. Kong, and A. Saaban, "Positivity preserving interpolation using rational bicubic spline," *J. Appl. Math.*, vol. 2015, Feb. 2015, Art. no. 572768.

[23] T. S. Shaikh, M. Sarfraz, and M. Z. Hussain, "Shape preserving constrained data visualization using rational functions," *J. Prime Res. Math.*, vol. 7, pp. 35–51, 2011.

[24] M. B. Walther and J. W. Schmidt, "Range restricted interpolation using Gregory's rational cubic splines," *J. Comput. Appl. Math.*, vol. 103, pp. 221–237, Mar. 1999.

[25] Y. Zhang, S. Gao, C. Zhang, and J. Chi, "Application of a bivariate rational interpolation in image zooming," *Int. J. Innov. Comput., Inf. Control*, vol. 5, no. 11, pp. 4299–4307, 2009.

[26] Y. Zhang, C. Zhang, H. Liu, and Q. Guo, "Region constraint of a bivariate rational interpolating surface," *Comput.-Aided Des. Appl.*, vol. 8, no. 6, pp. 809–818, 2011.

SAMSUL ARIFFIN ABDUL KARIM received the B.App.Sc., M.Sc., and Ph.D. degrees in computational mathematics and computer-aided geometric design (CAGD) from Universiti Sains Malaysia (USM). He is currently a Senior Lecturer with the Fundamental and Applied Sciences Department, Universiti Teknologi PETRONAS (UTP), Malaysia. He has been with the department for more than ten years. He had 20 years of experience using Mathematica and MATLAB software for teaching and research activities. He has published more than 120 papers in journal and conferences as well as seven books, including two research monographs, three edited conference volumes, and 20 book chapters. He has published one book in Springer Briefs in Energy: *Sustaining Electrical Power Resources through Energy Optimization and Future, Engineering* (Springer, 2018). His research interests include curves and surfaces designing, geometric modeling, and wavelets applications in image compression and statistics. He was a recipient of Effective Education Delivery Award and the Publication Award (Journal & Conference Paper), UTP Quality Day 2010–2012, respectively. He is a Certified WOLFRAM Technology Associate, Mathematica Student Level.

AZIZAN SAABAN received the bachelor's degree (Hons.) in applied sciences (computer technology), the M.Sc. degree in mathematics by research, and the Ph.D. degree in mathematics from Universiti Sains Malaysia. He is currently a Senior Lecturer and a Researcher with the Department of Mathematics, School of Quantitative Sciences, Universiti Utara Malaysia. His research interests include numerical method, geometric modeling, and computer-aided geometric design (CAGD), especially in practical application areas of scattered data interpolation.

VACLAV SKALA was a Professor with the University of West Bohemia (UWB), Pilsen. He has been with Brunel University London, U.K., Gavle University, Sweden, the Moscow Power Engineering Institute, Moscow, Russia, and others. He is also the Head of the Center of Computer Graphics and Visualization at UWB. He has published over 120 research indexed papers with more than 598 (Scopus) and 1579 (Scholar) citations. His current research interests include meshless (meshfree) methods for scalar and vector field approximation, fundamental algorithms and data structures for computer graphics and visualization, and geometry algebra application in computer graphics and geometry. He is also a Fellow of the Eurographics Association. He has been serving as an Associate Editor for prestigious research journals, such as *Computers and Graphics* (Elsevier), *The Visual Computer* (Springer), and *Computer Graphics Forum* (John Wiley & Sons.). He is also the Editor-in-Chief of the *Journal of WSCG*. He is active especially within computer graphics and visualization research communities and organizing research-oriented conferences, e.g., WSCG, GraVisMa, and HCI-Europe.